

# ACCURATE AND EFFICIENT, MULTISCALE SIMULATIONS OF NEWTONIAN AND NON-NEWTONIAN FREE-SURFACE FLOWS

JUAN LUIS PRIETO<sup>\*†</sup>, JAIME CARPIO<sup>†</sup>

<sup>†</sup> Departamento de Ingeniería Energética  
Escuela Técnica Superior de Ingenieros Industriales  
Universidad Politécnica de Madrid  
c/ José Gutiérrez Abascal, 2, 28006 Madrid, Spain  
e-mail: [juanluis.prieto@upm.es](mailto:juanluis.prieto@upm.es)  
ORCID<sup>®</sup> iD: [orcid.org/0000-0001-5085-0482](https://orcid.org/0000-0001-5085-0482)

**Key words:** Finite Element Method, Free-Surface, Multiscale, Adaptive Mesh Refinement, Non-Newtonian Flows

**Abstract.** The purpose of this presentation is to outline the main features of a new numerical method under development for the simulation of complex, Newtonian and non-Newtonian free-surface flows. The method makes use of a Particle Level Set (PLS) approach along with Adaptive Mesh Refinement (AMR) techniques to retrieve, accurately and efficiently, the fluid interface at each time step as the zero isocontour of a level set function. The convective terms are dealt with by means of a semi-Lagrangian formulation of the Navier-Stokes equations within a Finite Element framework, leveraging isotropic as well as anisotropic AMR techniques developed via error estimation to produce spatially-adapted “optimal” triangulations. Multiscale simulations of non-Newtonian flows are realized through the kinetic modelling of ensembles of dumbbells scattered over the domain, their internal configurations providing the extra-stress tensor representing the viscoelastic contribution to the Newtonian solvent.

The capabilities of the method are illustrated in a series of 2D simulations of pure-advection and complex free-surface flows, showing surface tension and viscoelastic effects.

## 1 INTRODUCTION

The development of a general, accurate, robust and efficient method for the solution of multiphase flows is a topic of great interest to the Scientific and Engineering community, due to the large number of applications in which a free-surface is present. Though in recent years significant progress has been made in this field [1, 2, 3] there is still much room for improvement; the purpose of this talk is to present a contribution in this

direction by means of a semi-Lagrangian Particle Level Set method with (An)Isotropic Mesh Refinement capabilities to capture the interface of pure advection and complex Newtonian and non-Newtonian flows, in a robust, accurate and efficient way.

## 2 METHODOLOGY

We briefly describe next the main features of the method introduced in this talk.

### 2.1 Time and space discretization

We take advantage of the semi-Lagrangian approach so that for each mesh-point, the departure points  $\mathbf{X}$  (or ‘feet’ of the characteristic curves) are computed according to:

$$\begin{cases} \frac{d\mathbf{X}(\mathbf{x}, t_n; t)}{dt} = \mathbf{u}(\mathbf{X}(\mathbf{x}, t_n; t), t), & t \in (t_{n-1}, t_n); \\ \mathbf{X}(\mathbf{x}, t_n; t_n) = \mathbf{x}. \end{cases} \quad (1)$$

Thus, the Navier-Stokes equations for incompressible, viscous flows can be rewritten in terms of a Stokes-like problem, in which quadratic finite elements are used for velocity, linear discontinuous for the pressure, and linear polynomials are employed for the level set function. Non-Newtonian fluids are considered by means of a multiscale procedure in which kinetic models are coupled with the macroscopic solution of the Navier-Stokes equations. The internal configurations  $\mathbf{Q}$  of the polymer particles advected by the flow are ruled by the stochastic differential equation:

$$d\mathbf{Q} = \left[ \kappa \cdot \mathbf{Q} - \frac{2}{\zeta} \mathbf{F}(\mathbf{Q}) \right] dt + \sqrt{\frac{4k_B\Theta}{\zeta}} d\mathbf{W}, \quad (2)$$

with  $\mathbf{F}$  the spring-force of the dumbbells,  $k_B$  the Boltzmann constant,  $\zeta$  the friction coefficient,  $\Theta$  the absolute temperature and  $\mathbf{W}$  a three-dimensional Wiener process. These configurations are conveniently integrated by a (weak) second-order scheme, with the polymer stress tensor being computed from their second moments. See [4, 5] for details.

### 2.2 Interface-capturing technique

The Particle Level Set method captures the interface as the zero isocontour of  $\phi$  (*level set function*) solving at each time step the conservation equation

$$\frac{D\phi}{Dt} = 0, \quad (3)$$

using the semi-Lagrangian approach sketched above. *Marker particles* advected by the flow and placed sufficiently close to the interface enhance shape reconstruction by defining local level set functions. A second-order accurate reinitialization procedure is also used to keep the level set function from developing numerical instabilities as the simulation goes on. For details, see the SLEIPNNIR technique introduced in [6].

### 2.3 Adaptive Mesh Refinement technique

Isotropic as well as anisotropic mesh refinement is here considered to produce spatially-adapted “optimal” triangulations as presented in [7, 8]. For isotropic mesh refinement one only has to define the size of elements  $|K| \propto h_K^d$  with any tolerance criterium: e.g.  $\min(h_K) = h_{\min}$ , to produce an equidistribution of the numerical error over all mesh elements. However, for anisotropic mesh refinement not only the size of the element must be provided, but also its shape  $S_K = \text{diag}\{s_{1,K}, \dots, s_{d,K}\}$  and orientation  $R_K = \{\mathbf{r}_{1,K}, \dots, \mathbf{r}_{d,K}\}$ . All this information is wrapped up in the so-called metric tensor, which is evaluated at each element of the spatial triangulation  $K$  as follows:

$$M_K = |K|^{-2/d} R_K S_K^{-1} R_K^T. \quad (4)$$

The optimal size of a given element  $|K|$  is computed via a posteriori error estimator of the truncation error incurred in each time subinterval  $[t_{n-1}, t_n]$ ; then, the optimal shape  $S_K$  and orientation  $R_K$  are determined using a linear a priori error analysis. 1269+

## 3 RESULTS

In this section we show some results obtained with our new method for the simulation of free-surface flows: first, we highlight the capabilities in pure advection problems, by means of the Zalesak slotted cylinder; then, we investigate bubble dynamics of Newtonian and non-Newtonian flows.

### 3.1 Advection problems

The test proposed by Zalesak [9] is carried out using our code with anisotropic mesh refinement active. This benchmark heavily taxes the ability of the free-surface method to accurately represent sharp interfaces, typically resulting in the interface-capturing or interface-tracking techniques rounding corners and eventually producing a degenerated free-surface after just a couple of solid body rotations.

**Table 1:** Minimum grid size  $h_{\min}^{-1}$ , number of elements  $NE$ , number of mesh-points  $NP$  and error in the infinity  $e_{L^\infty}$ , for the Zalesak slotted cylinder test after 50 revolutions, with anisotropic mesh refinement.

$h_{\min}^{-1}$	$NE$	$NP$	Error $e_{L^\infty}$
32	249	510	$1.02674 \times 10^{-3}$
64	486	983	$1.89065 \times 10^{-4}$
128	803	1616	$6.19143 \times 10^{-5}$
256	1053	2118	$3.26022 \times 10^{-5}$

The results for different minimum grid size  $h_{\min}$  with time step size  $\Delta t = 10^{-2}$ ,  $N_p = 5 \times 10^4$  marker particles and reinitialization of the level set function are collected in Table 1 after 50 revolutions of the slotted cylinder.

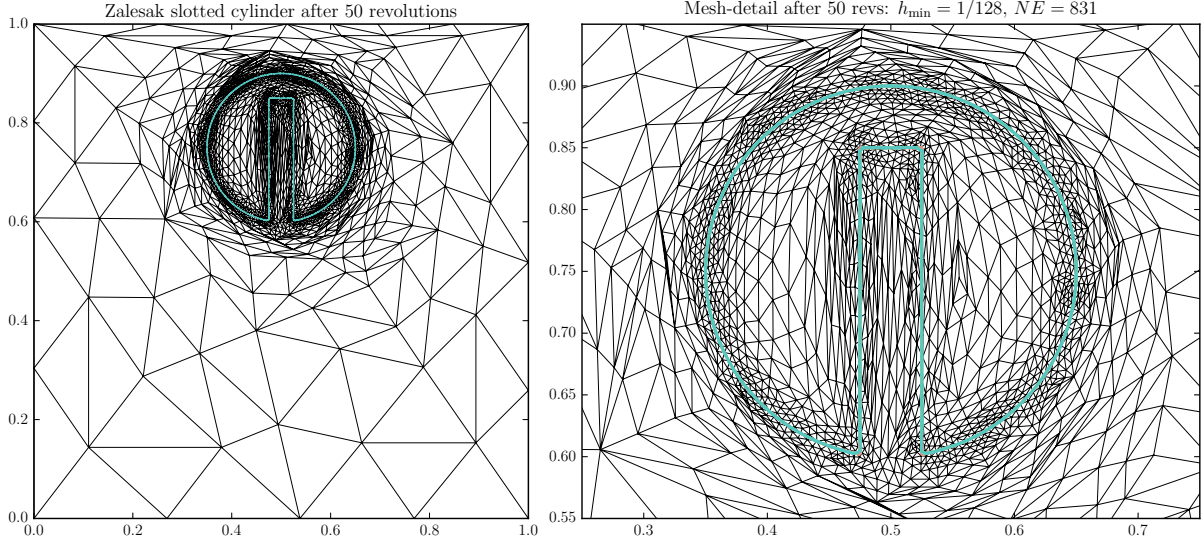


**Figure 1:** Zalesak slotted cylinder after 50 revolutions. Mesh with minimum grid size  $h_{\min} = 1/128$  and  $NE = 803$  elements. Time step size  $\Delta t = 10^{-2}$ ;  $N_p = 5 \times 10^4$  marker particles. Initial solution also plotted.

We observe very low errors in the infinity norm for a low number of elements  $NE$  and of mesh-points  $NP$ , along with an almost unchanged interface as plotted in Fig. 1, noticing that the initial interface quite overlaps the final shape when a mesh with as low as 803 elements are used.

### 3.2 Complex flows

We now move to more demanding problems with non-imposed flows. For this talk we consider the unsteady simulation of a bubble rising by buoyancy effects in a quiescent fluid. The Stokes problem derived from the semi-Lagrangian approach to the Navier-Stokes equations are solved efficiently using the PETSc (‘Portable, Extensible Toolkit for Scientific Computation’) tool [10], taking advantage of the PCFieldsplit approach based on the Schur-complement, block preconditioning of the Stokes matrix system.

In Fig. 2, we show the final shape of two such simulations along with isovelocity contours of the vertical component of the velocity over a contour-filled plot of that component  $v_y$ . The left panel of the Figure shows a Newtonian fluid rising in another Newtonian fluid, with moderate density and viscosity ratios  $\rho_2/\rho_1 = 10^{-1} = \mu_2/\mu_1$ , using  $N_p = 1.5 \times 10^3$  marker particles to improve shape preservation and prevent mass loss; surface tension effects are considered through the Weber dimensionless number ( $We = 35$ ), whereas the viscous and inertial effects are represented by the Reynolds number ( $Re = 35$ ); the time step size, in this mesh with minimum grid size  $h_{\min} = 1/320$ , is such that  $N_t = 960$  time steps are required to reach the dimensionless time  $t = 3$ , with an external mass loss of just  $1.7645 \times 10^{-5} \%$ . Under such conditions, the bubble reaches an ellipsoidal-cap

regime, which is in accordance with the findings of [11]. The right panel of Fig. 2 depicts a Newtonian bubble in a viscoelastic fluid represented by means of the FENE kinetic model, with the finite-extension parameter  $b_{FENE} = 35$ . This simulation scatters 15000 ensembles each of them containing 2500 dumbbells carrying the internal degrees of freedom of the polymer molecules. Compactly-Supported Radial Basis Functions (CSRBFs) are used as explained in [12] to reconstruct the extra-stress tensor that enters as a right-hand side term (body force) in the Navier-Stokes equations; this technique has proved extremely useful in AMR situations, where certain refined regions of the mesh have a low number of ensembles (or are empty of them altogether). The interface of the viscous-elastic ( $Re = 35$ ) bubble develops an incipient tail which due to surface tension effects ( $We = 50$ ) does not attain a cusp-like shape at the final time of the simulation; however, weak ‘negative’ (downwards) velocities are indeed observed in the wake of the bubble, something of a purely viscoelastic effect [13] which is here attained with a Deborah number  $De = 2.5$ .

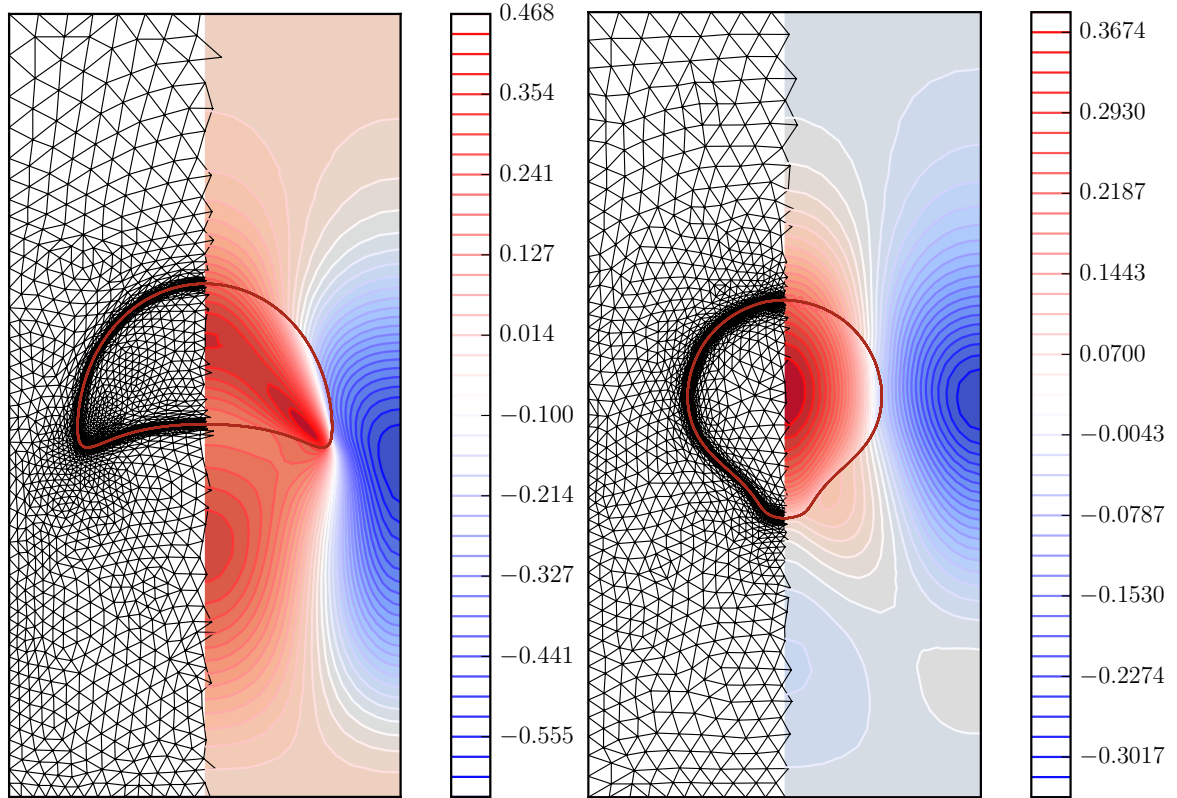


**Figure 2:** Bubble dynamics simulations at  $t = 3$  with isocontours of rise velocity: Newtonian fluid with  $Re = 35, We = 35$  (left panel); non-Newtonian fluid with  $b_{FENE} = 35, Re = 35, We = 50, c = 4.5, De = 2.5$  (right panel).

## 4 CONCLUSIONS

Next we collect some of the main points of the method under development presented in this talk:

- We present a new methodology for the simulation of free-surface flows for Newtonian and non-Newtonian flows.
- The method uses a Particle Level Set (PLS) approach along with Adaptive Mesh Refinement (AMR) techniques and the Finite Element Method.
- Pure advection problems are solved accurately even for extremely low number of mesh-points when using anisotropic mesh adaptation.
- Benchmark tests for complex flows both for Newtonian and non-Newtonian fluids show promising results: the simulations are carried out efficiently and accurately with the implementation of the new method.

## 5 ACKNOWLEDGMENTS

Financial support from project MTM2015-67030-P from Ministerio de Economía y Competitividad is acknowledged.

## REFERENCES

- [1] Larese, A., Rossi, R. and Oñate, E., Finite Element Modeling of Free Surface Flow in Variable Porosity Media. *Arch Computat Methods Eng.* (2015) **22**(4):637–653.
- [2] Cruchaga, M., Battaglia, L., Storti, M. and D’Elía, J., Numerical Modeling and Experimental Validation of Free Surface Flow Problems. *Arch Computat Methods Eng.* (2016) **23**(1):139–169.
- [3] Barral, N. and Olivier, G. and Alauzet, F., Time-accurate anisotropic mesh adaptation for three-dimensional time-dependent problems with body-fitted moving geometries. *J. Comput. Phys.* (2017) **331**:157–187.
- [4] Öttinger, H.C. *Stochastic Processes in Polymeric Fluids*. Springer, (1996), ISBN: 978-3-642-58290-5.
- [5] Prieto, J.L., Stochastic particle level set simulations of buoyancy-driven droplets in non-Newtonian fluids. *J. Non-Newtonian Fluid Mech.* (2015) **226**:16–31.
- [6] Prieto, J.L., SLEIPNNIR: A multiscale, particle level set method for Newtonian and non-Newtonian interface flows. *Comput. Methods Appl. Mech. Engrg.* (2016) **307**:164–192.

- [7] Carpio, J., Prieto, J.L. and Vera, M., A local anisotropic adaptive algorithm for the solution of low-Mach transient combustion problems. *J. Comput. Phys.* (2016) **306**:19–42.
- [8] Carpio, J. and Prieto, J.L., An anisotropic, fully adaptive algorithm for the solution of convection dominated equations with semi-Lagrangian schemes. *Comput. Methods Appl. Mech. Engrg.* (2014) **273**:77–99.
- [9] Zalesak, S.T., Fully multidimensional flux-corrected transport algorithms for fluids. *J. Comput. Phys.* (1979) **31**:335–362.
- [10] Balay, S., Abhyankar, S., Adams, M.F., Brown, J., Brune, P., Buschelman, K., Dalcin, L., Eijkhout, V., Gropp, W.D., Kaushik, D., Knepley, M.G., McInnes, L.C., Rupp, K., Smith, B.F., Zampini, S., Zhang, H. and Zhang, H. *PETSc Users Manual*. Argonne National Laboratory (2016), ANL-95/11 - Revision 3.7, <http://www.mcs.anl.gov/petsc>.
- [11] Clift, R., Grace, J.R. and Weber, M.E. *Bubbles, drops, and particles*. Academic Press, (1978), ISBN: 012176950X.
- [12] Prieto, J.L., An RBF-reconstructed, polymer stress tensor for stochastic, particle-based simulations of non-Newtonian, multiphase flows. *J. Non-Newtonian Fluid Mech.* (2016) **227**:90–99.
- [13] Chhabra, R. and De Kee, D.. *Transport Processes in Bubbles, Drops & Particles*, 2nd Ed.. Taylor & Francis, (2001).